

## Probing Hydrogen Bond Energies by Mass Spectrometry

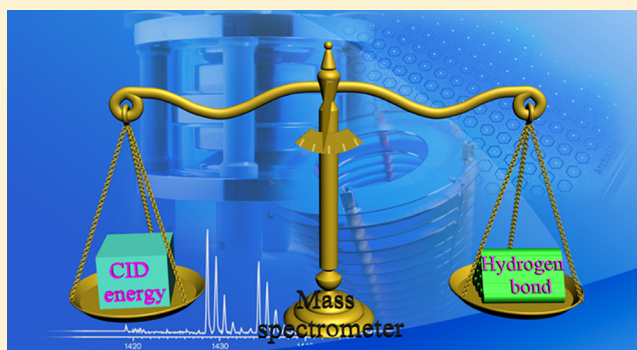
Hai-Feng Su,<sup>†</sup> Lan Xue,<sup>\*,‡</sup> Yun-Hua Li,<sup>†</sup> Shui-Chao Lin,<sup>†</sup> Yi-Mei Wen,<sup>†</sup> Rong-Bin Huang,<sup>†</sup> Su-Yuan Xie,<sup>\*,†</sup> and Lan-Sun Zheng<sup>†</sup>

<sup>†</sup>State Key Laboratory for Physical Chemistry of Solid Surfaces and Department of Chemistry, College of Chemistry and Chemical Engineering, Xiamen University, Xiamen 361005, China

<sup>‡</sup>Department of Chemistry, Ningde Normal University, Ningde 352100, China

### **S** Supporting Information

**ABSTRACT:** Mass spectrometry with desorption electrospray ionization (DESI) is demonstrated to be useful for probing the strength of hydrogen bonding, exemplified by various complexes of benzothiazoles and carboxylic acids in the solid state. Efficiencies for fragmentation of the complexes, quantified by collision-induced dissociation (CID) technology, correspond well with energies of the hydrogen bonds of O–H···N and N–H···O bridging each pair of benzothiazole and carboxylic acid. Linear correlations (with correlation factors of 0.8953 and 0.9928) have been established for the calibration curves of normalized collision energy at 100% fragmentation rate vs the length between donor and acceptor (in the hydrogen bond of O–H···N) as well as the slope of the fragmentation efficiency curve vs the average length difference between O–H···N and N–H···O in the complex. The mechanism responsible for determination of the hydrogen bonds is proposed on the basis of the experiments starting from the mixtures of the complexes as well as labeling with deuterium. As a complement of previously available methods (e.g., X-ray diffraction analysis), expectably, the proposed mass spectrometric method seems to be versatile for probing hydrogen bond energies.



### ■ INTRODUCTION

The concept of the hydrogen bond has been proposed for almost 100 years.<sup>1</sup> It is a class of attractive interaction<sup>2</sup> ubiquitous in materials and prevalent in inorganic, organic, supramolecular, biological, medicinal, and pharmaceutical chemistry.<sup>3–8</sup> The strength of the hydrogen bond, theoretically calculated to range from ~0.2 to 40 kcalmol<sup>-1</sup>,<sup>9</sup> has a critical impact on the physical or chemical properties of corresponding materials. For example, catalyzed reactions,<sup>10</sup> chelate cooperativity,<sup>11</sup> mechanical properties, and glass transition<sup>12</sup> are highly sensitive to the strength of the hydrogen bond. However, most of the available methods for determination of the hydrogen bond, such as NMR and IR spectroscopy, are far from quantification regarding hydrogen bond energies.<sup>9,13,14</sup> Historically, the shortening of distance between donor and acceptor determined by crystallographic data corresponds with the strength of hydrogen bond.<sup>2</sup> However, this empirical observation is true only for strong hydrogen bonds.<sup>2</sup> By crystallography (either X-ray or neutron diffraction), in addition, sensitivity and accuracy for determining interatomic distances and, in turn, the energies of hydrogen bond are highly dependent on crystal packing. The crystal packing is driven possibly by a combination of various intermolecular forces, e.g., hydrogen bond, halogen bond,  $\pi$ – $\pi$  interaction, or others. It is hard to distinguish the hydrogen bond from the other intermolecular forces by means of crystallography itself.

Therefore, an alternative method superior to crystallography for probing the hydrogen bond is highly desired.

Mass spectrometry (MS) is a versatile technique to characterize analytes based on mass-to-charge ratio ( $m/z$ ). The discovery of desorption electrospray ionization (DESI) allows direct and rapid MS analysis of various compounds in solid surfaces, free from redundant sampling preparation.<sup>15</sup> For example, DESI-MS had been applied for mapping analytes separated by thin-layer chromatography,<sup>16</sup> profiling biological tissue in situ,<sup>17,18</sup> imaging latent fingerprints,<sup>19</sup> determining SVOC in aerosols,<sup>20</sup> detecting reaction intermediates,<sup>21,22</sup> and tracing chemical reactions in the solid state directly.<sup>23–25</sup> However, the DESI-MS had never been developed for determining hydrogen bond, though strong hydrogen bonds between compounds in the spray and those on the surface were observed with reactive DESI.<sup>15,26,27</sup> Here we show that the DESI-MS is useful to probe the hydrogen bonds in the complexes of benzothiazoles and carboxylic acids. The proposed method, based on the correlation of the bond strength with the energy of collision-induced dissociation (CID) fragmentation, has been verified by various complexes of benzothiazole and carboxylic acid having typical hydrogen bonds of O–H···N and N–H···O.

Received: December 12, 2012

Published: April 3, 2013

## EXPERIMENTAL SECTION

**Materials.** 2-Aminobenzothiazole, 2-amino-4-methylbenzothiazole, 2-amino-6-methylbenzothiazole, 2-amino-6-methoxybenzothiazole, malonic acid, adipic acid, pimelic acid, octanedioic acid, azelaic acid, sebacic acid, and methanol-*d* were purchased from Alfa Aesar (Ward Hill, MA), HPLC-grade acetonitrile and methanol were purchased from TEDIA Co. (Fairfield, OH). Ethanol and cyclohexane were bought from Sinopharm Chemical Reagent Co. (Shanghai, China).

**Preparation of Crystals.** 2-aminobenzothiazole (75 mg, 0.5 mmol) and azelaic acid (94 mg, 0.5 mmol) were mixed in acetonitrile/H<sub>2</sub>O (10 mL, v/v = 1:1) in the presence of ammonia (0.5 mL) under ultrasonic treatment (160 W, 40 kHz, 50 °C). The resultant colorless solution was allowed to evaporate the solvent under 35 °C constant environment for one week to give colorless cocrystals of 2-aminobenzothiazole and azelaic acid (3, 2ABT·aze). The same procedure was conducted to obtain crystals/solids of 2-amino-4-methylbenzothiazole and adipic acid (1, 2A4MBT·adip), 2-amino-4-methylbenzothiazole and octanedioic acid (2, 2A4MBT·octa), 2-amino-6-methylbenzothiazole and azelaic acid (4, 2A6MBT·aze), 2-amino-6-methylbenzothiazole and adipic acid (5, 2A6MBT·adip), 2-amino-6-methoxybenzothiazole and malonic acid (6, 2A6MOBT·mal), 2-amino-6-methoxybenzothiazole and pimelic acid (7, 2A6MOBT·pim), and 2-amino-6-methoxybenzothiazole and sebacic acid (8, 2A6MOBT·seb).

All of the crystals were intentionally prepared on purpose of the present work. The experimental details for X-ray diffraction for these crystals are described in the Supporting Information.

**Mass Spectrometric Analysis.** DESI-MS experiments were carried out in the positive ion mode on a Bruker Esquire HCT ion trap mass spectrometer (Billerica, MA) coupled with a homemade DESI device. Parameters of the DESI source were optimized to enhance the signal intensity. Acetonitrile/cyclohexane/methanol 55:35:10 (v/v/v) were used as spray solvent at a flow rate of 0.24 mL/h. The angle between the DESI spray needle and the sample surface was set to 86°, and the tip-to-surface distance was set to 5 mm. The end of the MS-inlet capillary was about 1.5 cm from the sample. The capillary voltage was set to 4 kV. The pressure of nebulizing nitrogen, the flow rate of desolvation gas, and the temperature of desolvation gas were set to 60 psi, 4 L/min, and 200 °C, respectively. In the CID experiments, the collision gas was helium with a pressure of  $4 \times 10^{-6}$  mbar. The fragmentation time and fragmentation delay (interval between precursor ion isolation and fragmentation) were 40 and 0 ms, respectively. The solutions of the involved benzothiazoles and carboxylic acids were analyzed by electrospray ionization (ESI) mass spectrometry as well.

## RESULTS AND DISCUSSION

### Hydrogen Bonds Characterized by X-ray Diffraction.

Shown in Figure 1 are the five pairs of compounds 1–5 with hydrogen bonds characterized by X-ray crystallography (see the Supporting Information for the crystallographic data in detail). Clearly there are two typical hydrogen bonds, i.e., O–H···N and N–H···O in each pair of benzothiazole and carboxylic acid. As shown in Figure 1, both O–H···N and N–H···O in the complexes 1–5 form the hydrogen bonds with motif of R<sub>2</sub><sup>2</sup>(8), which is a widely accepted symbol to define the hydrogen bond.<sup>28</sup> Crystallographic data for 1–5 are listed in the Supporting Information (Table S1 and Figure S1). The lengths of the hydrogen bonds (O–H···N/N–H···O) between benzothiazole and carboxylic acid (referred as the lengths between the donor and the acceptor in this paper, as listed in Table 1 and shown in Figure S1, Supporting Information) are [2.690(2)/2.693(2), 2.893(2)/2.920(2)], [2.678(5)/2.696(4), 2.905(5)/2.935(5)], [2.636(3)/2.707(3), 2.975(3)/2.902(4)], [2.633(2), 2.941(2)], [2.598(2), 2.935(3)] Å for 1–5, respectively. (Note that there are two sets of O–H···N/N–H···O bonds at two ends of the carboxylic acid in 1–3 as

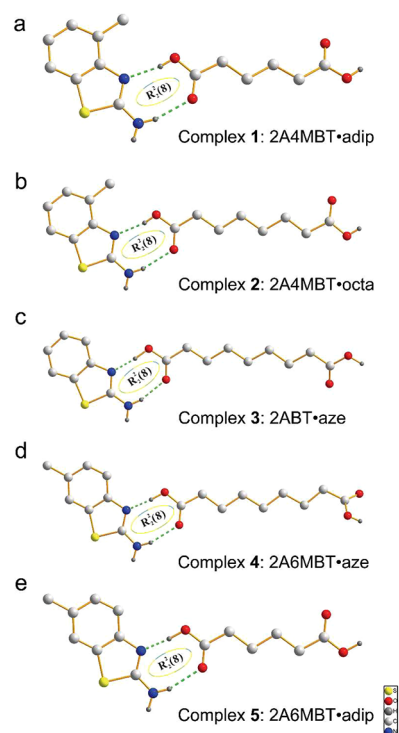


**Figure 1.** Hydrogen bond motifs in the cocrystals of 1–5 (a–e for 1–5, respectively). Hydrogen bonds are drawn as green dashed lines. The involved hydrogen atoms are theoretically added.

revealed by X-ray crystallography. The number in parentheses behind the determined bond lengths is the estimated standard deviation of the bond length.) The distances between the donors (O–H or N–H) and the acceptors (N or O) are much less than the sum of the van der Waals radii of O (1.43 Å), N (1.53 Å), and H (1.10 Å). Moreover, in geometric criteria the N–H donor (or the N acceptor) in the benzothiazole derivative matches very well with the O acceptor (or the O–H donor) in the partner carboxylic acid. The strong hydrogen bonds (N–H···O and O–H···N) in each complex of benzothiazole and carboxylic acid are matched to each other to such a degree that the aggregate consisting of one benzothiazole derivative and one carboxylic acid is just like a pair of key and lock. The strong and matchable hydrogen bonds of O–H···N and N–H···O lead to the complete same configuration of R<sub>2</sub><sup>2</sup>(8) motif in each pair of complex.

As the electronegativity of O is higher than N, the O–H group of carboxylic acid renders a stronger donor than the N–H group of amino, and the heterocyclic nitrogen atom renders a stronger acceptor than the oxygen atom in C=O group of carboxylic acid.<sup>9</sup> As expected, the length of O–H···N, between a stronger donor and a stronger acceptor, is shorter than that of N–H···O in each complex involved. The shortest hydrogen bond lengths in 1–5 are 2.690, 2.678, 2.636, 2.633, and 2.598 Å (Table 1), respectively, indicating the bond length of O–H···N in 1–5 decreases sequentially and, in turn, the strength of hydrogen bond increases in the order from 1 to 5.

**Hydrogen Bonds Characterized by Mass Spectrometry.** Figure 2 shows the mass spectra analyzed by DESI-MS and ESI-MS for the cocrystals of benzothiazoles and carboxylic acids in the solid state and in the solution, respectively. Taking complex 4 as an example, the DESI-MS spectrum (Figure 2d) presents the protonated 2-amino-6-methylbenzothiazole (*m/z*

Table 1.  $m/z$  and Hydrogen Bond Lengths of Compounds 1–5

complex	$m/z$ value	hydrogen bond lengths (Å)	avg length of O–H...N (Å)	avg length of N–H...O (Å)	shortest hydrogen bond length (Å)	avg length difference between O–H...N and N–H...O (Å)
1 2-amino-4-methylbenzothiazole and adipic acid	311.1	[2.690(2)/2.693(2), 2.893(2)/2.920(2)]	2.692	2.907	2.690	0.215
2 2-amino-4-methylbenzothiazole and octanedioic acid	339.1	[2.678(5)/2.696(4), 2.905(5)/2.935(5)]	2.687	2.920	2.678	0.233
3 2-aminobenzothiazole and azelaic acid	339.1	[2.636(3)/2.707(3), 2.975(3)/2.902(4)]	2.672	2.939	2.636	0.267
4 2-amino-6-methylbenzothiazole and azelaic acid	353.2	[2.633(2), 2.941(2)]	2.633	2.941	2.633	0.308
5 2-amino-6-methylbenzothiazole and adipic acid	311.1	[2.598(2), 2.935(3)]	2.598	2.935	2.598	0.337

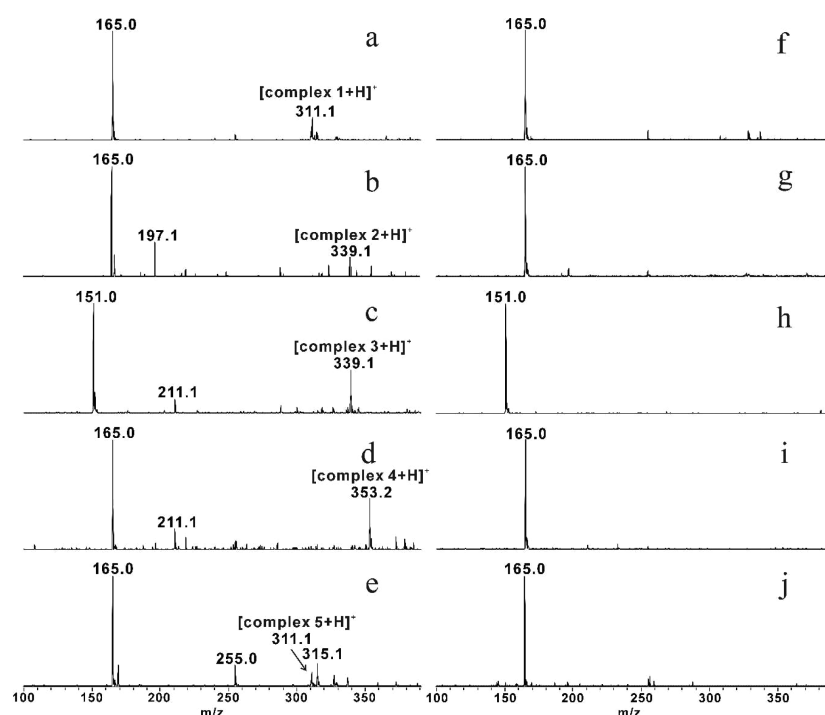


**Figure 2.** Mass spectra of 1–5 characterized by DESI-MS (a–e for 1–5, respectively) in the solid state and ESI-MS (f–j for 1–5, respectively) in the solution.

165) and the sodium complex of azelaic acid ( $m/z$  211). Specifically, the signal at  $m/z$  353 is assignable to the complex of 2-amino-6-methylbenzothiazole and azelaic acid (2A6MBT·aze) bridged by hydrogen bonds. By contrast, in regular ESI-MS analysis (Figure 2i) with the complex of 2A6MBT·aze being dispersed by the solvent, the signal of  $m/z$  353 is missing because the complex structure of 2A6MBT·aze is destroyed by reorganization of the hydrogen-bonded complex in solution.<sup>29</sup>

Analogous phenomena were observed in corresponding DESI-MS and ESI-MS for each cocrystal of 1, 2, 3, or 5. The protonated ions of 2A4MBT and 2A4MBT·adip ( $m/z$  165 and 311), 2A4MBT and 2A4MBT·octa ( $m/z$  165 and 339), 2ABT and 2ABT·aze ion ( $m/z$  151 and 339), and 2A6MBT and 2A6MBT·adip ( $m/z$  165 and 311), in addition to a few sodium complexes of partner carboxylic acids, were observed in the DESI-MS analyses (Table 1 and Figure 2a,b,c,e). By contrast, the ESI-MS of 1, 2, 3, and 5 predominately show the protonated 2A4MBT, 2A4MBT, 2ABT, and 2A6MBT ( $m/z$  165, 165, 151, and 165 in Figure 2f,g,h,j, respectively). At a concentration higher than 0.025 mg/mL, the ESI-MS signal of

the complex such as 2ABT·aze ion ( $m/z$  339) is detectable (see the Supporting Information for the details). Accordingly, detection of hydrogen-bonded complexes is possible by ESI-MS at higher concentration. However, such a high concentration is unusual for a regular ESI-MS analysis. These evidence collectively demonstrate that DESI-MS (in principle having higher concentration of analytes in the initially formed droplets) is better than regular ESI-MS for identifying hydrogen bonding complexes.

To establish the mechanism responsible for hydrogen-bonded complexes determined by the DESI-MS, two pristine crystals (complexes 1 and 3) were simultaneously characterized in three kinds of mixtures in the solid state (Figure 3, the experimental details are described in the Supporting Information in which mixtures of complexes 2 and 3 are exemplified). If complexes 1 and 3 underwent decomposition in the DESI-MS process, the benzothiazoles (2-amino-4-methylbenzothiazole and 2-aminobenzothiazole) and the carboxylic acids (adipic acid and azelaic acid) in 1 and 3 would suffer in reassembly to possibly produce new complexes rather than 1 and 3. The mass spectrum (Figure 3a) of the



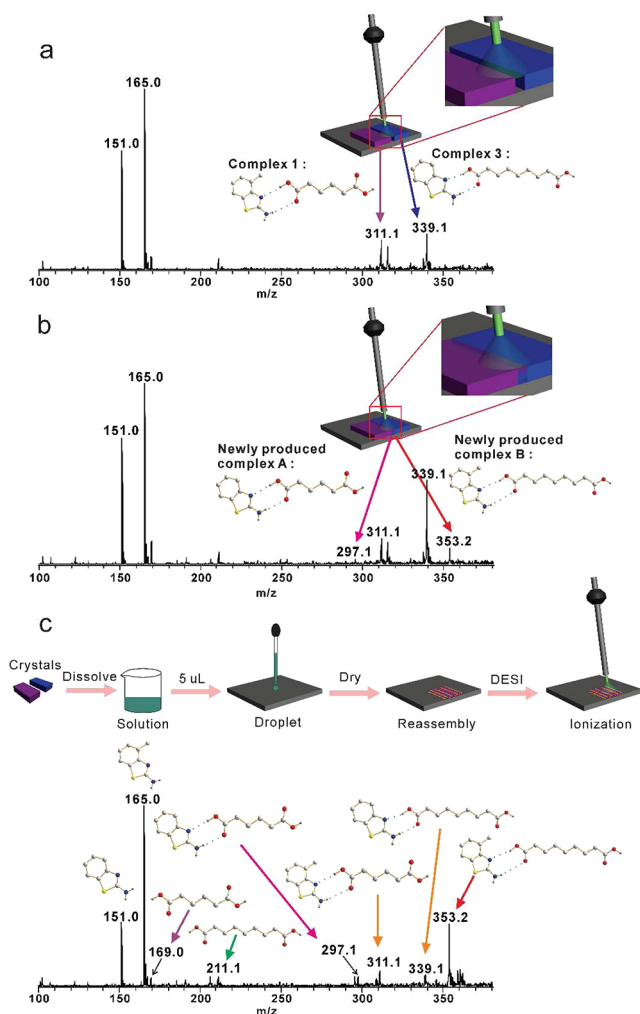


**Figure 3.** Mass spectra and experimental illustrations of DESI-MS for the mixture of **1** and **3** (a, pristine crystals of **1** and **3** setting closely; b, pristine crystals of **1** and **3** setting overlap; c, solids recrystallized from the acetonitrile/H<sub>2</sub>O solution of **1** and **3**).

samples with two pristine crystals of **1** and **3** setting close to each other (but no contact or overlap) seems to be the simple combination of the individual mass spectrum of **1** (Figure 2a) plus **3** (Figure 2c). As shown in Figure 3b, however, two new signals of  $m/z$  297 and 353, assignable to the complex of 2-aminobenzothiazole and adipic acid (complex A) as well as the complex of 2-amino-4-methylbenzothiazole and azelaic acid (complex B), respectively, in addition to the original  $m/z$  311 (for complex **1**) and  $m/z$  339 (for complex **3**) are clearly detected by DESI-MS for the samples of two pristine crystals setting overlap. This spectrum (Figure 3b) with unbalanced signals of  $m/z$  297 and 353 is similar to that of the solid analytes produced by recrystallization from acetonitrile/H<sub>2</sub>O solution of **1** and **3** (Figure 3c), implying the hydrogen-bonded complexes determined by the proposed DESI-MS undergo the similar process, typically including solution, droplet, reassembly, and ionization as shown in the illustration of Figure 3c. Accordingly, we tentatively assume the mechanism responsible for identification of the hydrogen-bonded complexes is similar to a typical DESI-MS process previously discussed in literatures.<sup>30–32</sup> The crystal surface is wetting to form a droplet-thin film<sup>30</sup> in the solvent spray, then the complexes of benzothiazoles and carboxylic acids are dissolved in the droplet-

thin film and subject to the “droplet pick-up”<sup>31</sup> or liquid–solid microextraction<sup>32</sup> into droplets, followed by solvent evaporation leading to reassembly of the benzothiazole(s) and the carboxylic acid(s) and formation of dry ions of complexes during droplet transfer to the mass spectrometer. We speculate the analytes are neutral in the course of transfer (i.e., first three stages, solution, droplet, and reassembly) but ionized in the latter stage of droplet evaporation. Our deuterium-labeled ESI-MS/MS experiment clearly exemplifies that the heterocyclic nitrogen would be protonated to prevent formation of the O–H...N hydrogen bond and detection of the hydrogen-bonded complexes if individual benzothiazole was ionized in the first three stages (vide infra).

The MS signals of the complexes recorded in the present experiments are the protonated species. In principle, there are two positions susceptible to protonation in the benzothiazole, i.e., the nitrogen atom in the thiazole ring or the amino group. The hydrogen bond is viable if a proton was added in the amino group, but the hydrogen bond of O–H...N would be dissociated if the protonation was occurred in the heterocyclic nitrogen atom. To prove the hydrogen-bonded complex tolerable in the DESI-MS analysis, therefore, it is necessary to know where the proton is attached in the complex species during the DESI ionization process. A series of deuterium-labeled tandem DESI-MS or ESI-MS experiments with 2-amino-6-methylbenzothiazole or **4** (the complex of 2-amino-6-methylbenzothiazole and azelaic acid) were designed to confirm the location of proton in the complex of benzothiazole and carboxylic acid. As shown in Figure 4a, ions of  $m/z$  150,

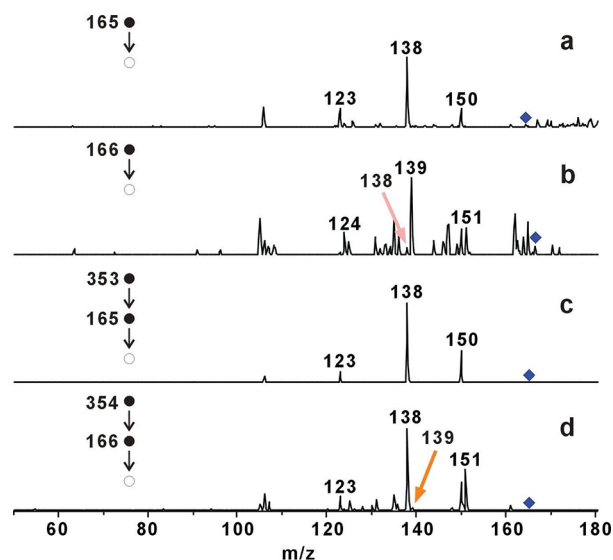
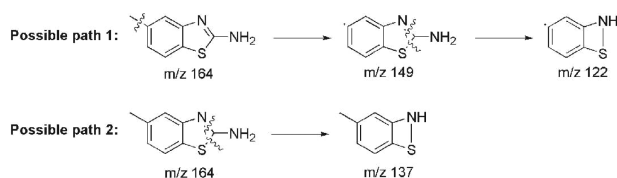


**Figure 4.** Tandem mass spectra of 2-amino-6-methylbenzothiazole and **4** acquired by ESI-MS and DESI-MS (a and b, ESI-MS/MS of 2-amino-6-methylbenzothiazole with CH<sub>3</sub>OH and CH<sub>3</sub>OD as solvent, respectively; c and d, tandem DESI-MS of **4** with CH<sub>3</sub>OH and CH<sub>3</sub>OD as solvent, respectively).

138, and 123 were generated as the major fragments starting from the precursor ion of protonated 2-amino-6-methylbenzothiazole ( $m/z$  165) in the ESI-MS/MS experiment with methanol as solvent. These ions are assignable to the fragmentation of protonated 2-amino-6-methylbenzothiazole by loss of CH<sub>3</sub>, CNH, or CH<sub>3</sub> + CNH (as shown in the possible path 1 for CH<sub>3</sub> and CH<sub>3</sub> + CNH, possible path 2 for CNH in Scheme 1). The CNH group is reasonably derived

### Scheme 1. Possible Paths for the Dissociation of 2-Amino-6-methylbenzothiazole



from the amino group (rather than the heterocyclic nitrogen) due to structural and compositional similarity. Considering the same fragments ( $\text{CH}_3$ ,  $m/z$  15;  $\text{CNH}$ ,  $m/z$  27; and  $\text{CH}_3 + \text{CNH}$ ,  $m/z$  42) losing in the deuterium-labeled ESI-MS experiment with  $\text{CH}_3\text{OD}$  in replacement of  $\text{CH}_3\text{OH}$  as solvent (Figure 4b), it is reasonable to conclude that the proton/deuterium ion retains in the nitrogen atom of the heterocyclic ring of 2-amino-6-methylbenzothiazole during the ESI-MS/MS process. Otherwise, the dominated fragments signals should be  $m/z$  151, 138, and 123 corresponding to loss of  $\text{CH}_3$ ,  $\text{CND}$ , and  $\text{CH}_3 + \text{CND}$ .

For the tandem DESI-MS experiment with **4** as analyte and  $\text{CH}_3\text{OH}$  as solvent, the signals of  $m/z$  150, 138, and 123 were detected (Figure 4c). By contrast, the predominated products of  $m/z$  151, 138, and 123 are shown in Figure 4d, which were assigned to the loss of  $\text{CH}_3$ ,  $\text{CND}$ , and  $\text{CH}_3 + \text{CND}$  from the parent ions of  $m/z$  166 (deuterated 2-amino-6-methylbenzothiazole fragmented from complex **4**) in the tandem DESI-MS experiment with  $\text{CH}_3\text{OD}$  as solvent. The conflicting evidence in the deuterium-labeled ESI-MS/MS (for 2-amino-6-methylbenzothiazole) and tandem DESI-MS (for **4**) indicate the amino might be the right group for protonation/deuterated and, in turn, fragmented as  $\text{CNH}/\text{CND}$  to leave from the precursor ions of 2-amino-6-methylbenzothiazole in **4** during the tandem DESI-MS process. These data corroborate that the ionization of hydrogen-bonded complex necessary for mass spectrometric analysis does not influence survival of the hydrogen bonds,  $\text{O}-\text{H}\cdots\text{N}$  and  $\text{N}-\text{H}\cdots\text{O}$ . In this case, the nature of donor and acceptor in the hydrogen bonds of  $\text{O}-\text{H}\cdots\text{N}$  and  $\text{N}-\text{H}\cdots\text{O}$  is not changed at all during the ionization process. It is well-known the strength of hydrogen bond is mainly influenced by the electronegativity of donor and acceptor.<sup>2</sup> Accordingly, the present protonated complexes having the same donors/acceptors with neutral ones are reasonable to have approximately similar hydrogen bond strength with the neutral complexes. However, detailed influence of the protonation on the hydrogen bond energies remains to be investigated theoretically.

In principle, hydrogen transfer between the amino group and the heterocyclic nitrogen atom is unavoidable during the mass spectrometric process. As shown in Figure 4b, for example, the weak signal of  $m/z$  138 is produced together with  $m/z$  139. It is almost certainly due to the hydrogen/deuterium transfer between the amino group and the deuterated heterocyclic nitrogen atom in the deuterium-labeled ESI-MS/MS experiment of 2-amino-6-methylbenzothiazole. As the peak area of the  $m/z$  138 is about 8% of the  $m/z$  139, the probability for such a hydrogen/deuterium transfer seems rather slight. Similar transfer is also recorded in the deuterium-labeled tandem DESI-MS experiment for **4** (Figure 4d), in which the weak signal of  $m/z$  139 in addition to the predominated  $m/z$  138 is shown to demonstrate the slight hydrogen/deuterium transfer

from deuterated amino group to the heterocyclic nitrogen atom.

**Quantifying Hydrogen Bond by DESI-MS with CID Fragmentation.** To quantify the hydrogen bonds, a CID experiment was further performed. The CID technique allows fragmentation of the hydrogen-bonded complex so as to identify the strength of hydrogen bond depending on the relationship between collision energy and fragmentation signal. In such a CID process, the electronics system in the instrument generates a broadband frequency spectrum with all resonating frequencies presented except for the frequency corresponding to the resonance of the target ion, isolating it for further analysis. After that, the energy of the target ion is increased by resonance excitation from the dipole field, and the resonating ions quickly take in energy from the dipolar field, collide with the helium background gas, and then dissociate to create a predictable and reproducible mass spectrum. Taking **2** as an example (Figure 5), a fragment from the complex of

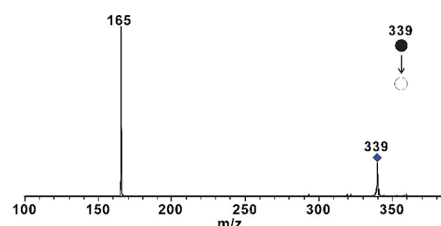


Figure 5. Mass spectrum of **2** acquired in a CID collision energy.

2A4MBT-octa can be detected in MS with a CID experiment. The relative intensity of the fragment vs parent ions is changeable depending on the collision energy. Although the actual energy of precursor ions colliding with the helium background gas is hard to simulate under currently experimental conditions, the dissociation energy can be evaluated relative to the amplitude of the excitation in the CID process.<sup>33</sup>

Figure 6 shows the fragmentation efficiency curves for the five kinds of complexes. The meaningful curve is plotted by the

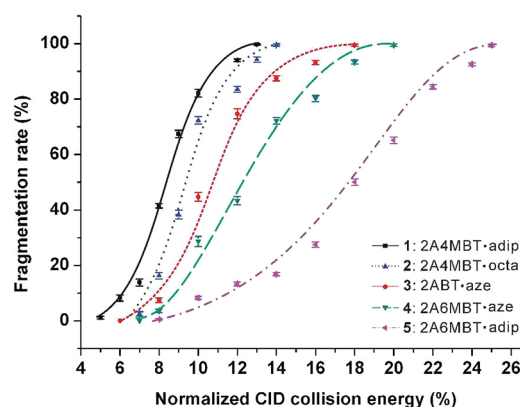
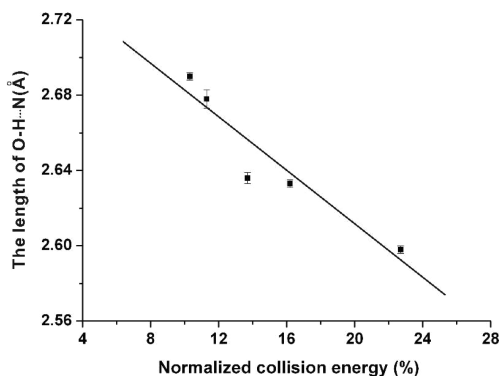


Figure 6. Fragmentation efficiency curves for complexes **1**–**5**.

fragmentation rate [the ratio of fragment intensity vs total (parent plus fragment) intensities of MS signals in such as Figure 5] against normalized collision energy (%) for each complex.<sup>34</sup> In such a curve, the 100% fragmentation represents the case with the hydrogen bond completely dissociated. The final bond broken during the fragmentation process is in

principle the shortest hydrogen bond in the complex, so it is reasonable to connect the collision energy at the point of 100% fragmentation to the shortest hydrogen bond in corresponding complex. The slope of the curve meets 100% fragmentation rate at 10.3%, 11.3%, 13.7%, 16.2%, and 22.7% for 1–5, respectively (see the Supporting Information for the evaluation in detail). These data suggest the relative energy for dissociation of the hydrogen bond in the sequence from 1 to 5. As expected, the values of relative dissociation energy at 100% fragmentation correspond well with the shortest of lengths between donor and acceptor (O–H···N) in the crystals (2.690, 2.678, 2.636, 2.633, and 2.598 Å for 1–5, respectively, as listed in Table 1). As shown in Figure 7, the calibration curve with well correlation equation (eq A:  $y = 2.754 - 0.007x$ ) of normalized collision energy (%) at 100% fragmentation rate vs the length of O–H···N is obtained.



**Figure 7.** Correlation between the length of O–H···N (Å) and the normalized collision energy (%) at 100% fragmentation rate.

Additionally, the slope of the fragmentation efficiency curve corresponds to the discrepancy of the two involved hydrogen bonds, i.e., difference between the shorter O–H···N bond and the longer N–H···O bond in the present cases. In principle, the complex fragmentizes starting from the weaker bond (N–H···O) and completing at stronger one (O–H···N). In the fragmentation efficiency curve, statistically, the 100% fragmentation represents the broken of the stronger bond (O–H···N), whereas the starting inflection point of the fragmentation curve corresponds to the dissociation of weaker hydrogen bond (N–H···O). Therefore, the slope of the fragmentation efficiency curve increases with the decrease of difference between the shorter hydrogen bond and the longer one. For the present complexes 1–5, the average difference between the bonds of longer N–H···O and the shorter O–H···N are 0.215, 0.233, 0.267, 0.308, and 0.337 Å, respectively, according to the crystallographic data (Table 1). As shown in Figure 8, indeed, these values correspond well with the slopes of the fragmentation efficiency curves (23.8, 22.2, 17.2, 12.7, and 10.0 for complexes 1–5, respectively). The correlation of the slope of the fragmentation efficiency curve vs the average difference of the hydrogen bond between O–H···N and N–H···O is quantified as the equation of  $y = 48.9 - 116.6x$  (eq B).

The errors for the data of fragmentation rate are less than 5% (as illustrated in Figure 6), and the correlation factors for the calibration curves (Figures 7 and 8) are 0.8953 (for eq A) and 0.9928 (for eq B). Although the meaningful implications regarding the equation parameters remain to be further explored, sensitivity and accuracy of the proposed method are

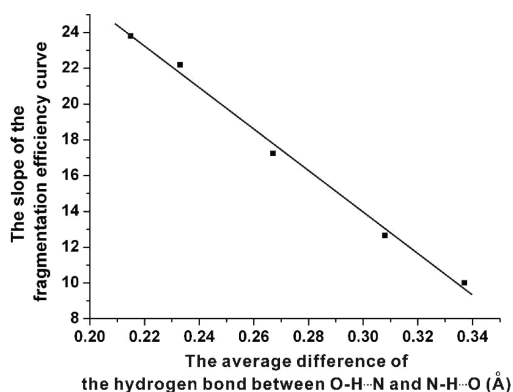


**Figure 8.** Correlation between the slope of the fragmentation efficiency curve and the average difference of the hydrogen bond between O–H···N and N–H···O (Å).

high enough to quantify the relative strength of hydrogen bonds at least in the discussed complexes.

**Comparison of the Proposed Method with Crystallography for Probing the Hydrogen Bond.** Based on the two equations (A and B), the dissociation energy can be relatively quantified according to a given hydrogen bond length (between donor and acceptor) or reversed. Three kinds of analogue complexes of 2-amino-6-methoxybenzothiazole with malonic acid (6, 2A6MOBT·mal), pimelic acid (7, 2A6MOBT·pim), and sebacic acid (8, 2A6MOBT·seb) were selected to validate the proposed method. The fragmentation efficiency curves for the three kinds of cocrystals (6–8) are shown in Figure 9. The slopes of the fragmentation efficiency curves are

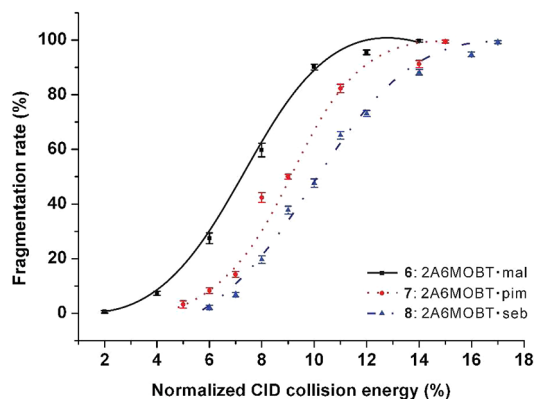


**Figure 9.** Fragmentation efficiency curves for complexes 6–8.

16.1, 18.2, and 12.9 and meet 100% fragmentation rates at 10.3%, 11.8%, and 14.0%, respectively. Calculated by the calibration curves (eqs A and B), the data suggest the lengths of hydrogen bonds (O–H···N, N–H···O) are (2.682, 2.963), (2.671, 2.934), and (2.656, 2.965) Å for 6–8, respectively.

We have attempted to analyze the X-ray crystallographic data of 6–8 for checking the hydrogen bond values suggested by DESI-MS. With the exception of 7, crystals of 6 and 8 were grown and the lengths between benzothiazoles and carboxylic acids (O–H···N, N–H···O) were measured as [2.701(3), 2.833(3)] and [2.649(4), 3.057(5)] Å for 6 and 8, respectively (the details of the hydrogen bonds and crystallographic data are listed in Table S1 and Figure S2 of the Supporting Information). Obviously, the mass spectrometric data are consistent with X-ray crystallography for the length of O–



H...N in **8**. However, the crystallographic data about the length of N–H...O (3.057 Å) in **8** and the lengths of O–H...N (2.701 Å) and N–H...O (2.833 Å) in **6** mismatch with those obtained from MS [2.965 Å for the N–H...O in **8** and (2.682, 2.963 Å) for the hydrogen bonds in **6**]. For **8**, the longer N–H...O length shown in the X-ray crystallographic data (0.092 Å longer than that obtained by MS) is likely due to the effect involved in the long chain of sebacic acid (longer than those in the other steric carboxylic acids of the discussed complexes **1–7**) in the crystal of **8**. The additional intermolecular force with respect to hydrogen bond such as N–H...O is survivable in crystal with numerous molecules assembled together (for crystallographic analysis) but unviable in the gas phase where the hydrogen-bonded complex exists as a two-molecule assembly of benzothiazole and carboxylic acid (for MS analysis). With regard to **6**, the length differences (0.019, –0.130 Å differences) of hydrogen bonds determined by MS and X-ray crystallography are likely caused by the proton transfer in the R<sub>2</sub><sup>2</sup>(8) moiety of the cocrystal **6**. It is well-known that hydrogen bonds are possibly involved in proton-transfer reactions.<sup>2</sup> As shown in Figure 10, the distance of C11–O4 (1.24 Å) in **6** is obviously

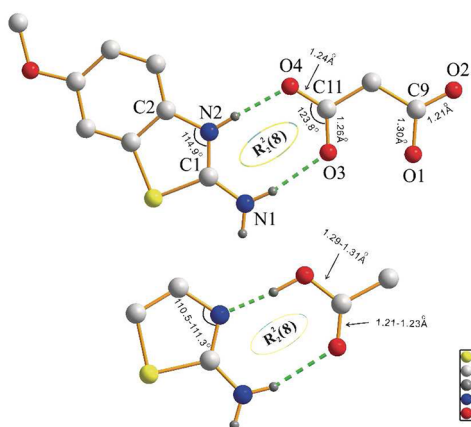


**Figure 10.** Hydrogen-bonded complex of **6** (top) and the corresponding hydrogen bond motifs in **1–5** and **8** (down).

shorter than those shown in the other complexes (**1–5** and **8**, 1.29–1.31 Å). This length difference indicates the hydrogen lost from O4 leading to the formation of double bond between C11 and O4. At the other end, the angle of C1–N2–C2 is enlarged to 114.9° from 110.5 to 111.3° (shown in **1–5** and **8**) with implication of hydrogen addition in N2. These evidence convergently prove the proton transfer from O4 to N2 in the R<sub>2</sub><sup>2</sup>(8) moiety, which results in the transformation of hydrogen bond from shorter O4–H...N2 into longer N2–H...O4 and leads to a slight change of the N1–H...O3 bond. Therefore, the complex of **6** exemplifies the hydrogen bond of O–H...N changed into N–H...O, and the crystallographic data about bond lengths of N–H...O and O–H...N in **6** are unreliable for quantifying the real strength of hydrogen bond. By contrast, the species detected by MS can be pure complexes having typical hydrogen bonds because the lifetime of the proton transfer is too short to be recorded by MS in the gas phase.<sup>35</sup> This experimental evidence about complexes **6–8** exemplifies that hydrogen bonds can be detected by mass spectrometry even without reliable X-ray crystallographic data and the innovative MS approach is thus a complement of the X-ray crystallographic method for probing hydrogen bonds.

## CONCLUSIONS

In this work, we propose a mass spectrometric method, based on DESI-MS with CID fragmentation, for probing the hydrogen bonds in the five pairs of selected complexes of benzothiazoles and carboxylic acids (**1–5**). The strengths of the hydrogen bonds between the benzothiazoles and the carboxylic acids (O–H...N and N–H...O) determined by X-ray crystallography are well correlated with the slope of the fragmentation efficiency curves and the collision energy of CID at a 100% fragmentation rate in the fragmentation efficiency curves of the corresponding mass spectra. In particular, the mass spectrometry is a complement of X-ray crystallography for probing hydrogen bonds because of some unavoidably additional forces in the crystal to influence the accurateness of crystallographic data. With potentially versatile applicability, the proposed mass spectrometric method is a heretofore unknown approach for hydrogen bond detection and is highly expected to be developed as a routine technology for quantifying hydrogen bonds in the future. The process supposed for DESI-MS identification of the hydrogen-bonded undergoes four stages, i.e., solution, droplet, reassembly, and ionization in turn. Although the possibility of determining hydrogen bonds in other systems (rather than the complexes of benzothiazoles and carboxylic acids) by mass spectrometry remains to be explored, starting from the present concept future ambition using innovative mass spectrometry to probe hydrogen bonds or any other weak bonds in various molecular assemblies may be stimulated.

## ASSOCIATED CONTENT

### Supporting Information

X-ray diffraction experiments, crystallographic data, ESI-MS of **3** with different concentrations, mass spectrometric experiments of DESI-MS for the mixtures of **2** and **3**, and the method for acquiring data from the fragmentation efficiency curve. This material is available free of charge via the Internet at <http://pubs.acs.org>.

## AUTHOR INFORMATION

### Corresponding Author

[syxie@xmu.edu.cn](mailto:syxie@xmu.edu.cn); [xxll654321@sina.com](mailto:xxll654321@sina.com)

### Notes

The authors declare no competing financial interest.

## ACKNOWLEDGMENTS

This work was supported by the NNSF of China (Grant Nos. 21031004, 21021061, and U1205111).

## REFERENCES

- (1) Pauling, L. *The Nature of the Chemical Bond*, 3rd ed.; Cornell University Press: Ithaca, 1963.
- (2) Arunan, E.; Desiraju, G. R.; Klein, R. A.; Sadlej, J.; Scheiner, S.; Alkorta, I.; Clary, D. C.; Crabtree, R. H.; Dannenberg, J. J.; Hobza, P.; Kjaergaard, H. G.; Legon, A. C.; Mennucci, B.; Nesbitt, D. J. *Pure Appl. Chem.* **2011**, *83*, 1637.
- (3) Lehn, J. M. *Supramolecular Chemistry. Concepts and Perspectives*; Wiley-VCH: Weinheim, 1995.
- (4) Schneider, H. J. *Angew. Chem., Int. Ed.* **2009**, *48*, 3924.
- (5) Falvello, L. R. *Angew. Chem., Int. Ed.* **2010**, *49*, 10045.
- (6) (a) Mukherjee, A. J.; Zade, S. S.; Singh, H. B.; Sunoj, R. B. *Chem. Rev.* **2010**, *110*, 4357. (b) Takahashi, O.; Kohno, Y.; Nishio, M. *Chem. Rev.* **2010**, *110*, 6049.

- (7) Ghosh, A. K.; Anderson, D. D.; Weber, I. T.; Mitsuya, H. *Angew. Chem., Int. Ed.* **2012**, *51*, 1778.
- (8) Gong, B. *Acc. Chem. Res.* **2012**, *45*, 2077.
- (9) Steiner, T. *Angew. Chem., Int. Ed.* **2002**, *41*, 48.
- (10) Lin, S.; Jacobsen, E. N. *Nat. Chem.* **2012**, *4*, 817.
- (11) Hunter, C. A.; Misuraca, M. C.; Turega, S. M. *J. Am. Chem. Soc.* **2011**, *133*, 20416.
- (12) Kharlampieva, E.; Kozlovskaya, V.; Sukhishvili, S. A. *Adv. Mater.* **2009**, *21*, 3053.
- (13) Jeffrey, G. A. *An Introduction to Hydrogen Bonding*; Oxford University Press: Oxford, 1997.
- (14) Schuster, P.; Zundel, G.; Sandorfy, C. *The Hydrogen Bond: Recent Developments in Theory and Experiments, Vol. 2: Structure and Spectroscopy*; North Holland: Amsterdam, 1976.
- (15) Takats, Z.; Wiseman, J. M.; Gologan, B.; Cooks, R. G. *Science* **2004**, *306*, 471.
- (16) Van Berkel, G. J.; Ford, M. J.; Deibel, M. A. *Anal. Chem.* **2005**, *77*, 1207.
- (17) Wiseman, J. M.; Ifa, D. R.; Zhu, Y. X.; Kissinger, C. B.; Manicke, N. E.; Kissinger, P. T.; Cooks, R. G. *Proc. Natl. Acad. Sci. U.S.A.* **2008**, *105*, 18120.
- (18) Eberlin, L. S.; Liu, X. H.; Ferreira, C. R.; Santagata, S.; Agar, N. Y. R.; Cooks, R. G. *Anal. Chem.* **2011**, *83*, 8366.
- (19) Ifa, D. R.; Manicke, N. E.; Dill, A. L.; Cooks, R. G. *Science* **2008**, *321*, 805.
- (20) Chen, H.; Li, M.; Zhang, Y. P.; Yang, X.; Lian, J. J.; Chen, J. M. *J. Am. Soc. Mass Spectrom.* **2008**, *19*, 450.
- (21) Perry, R. H.; Splendore, M.; Chien, A.; Davis, N. K.; Zare, R. N. *Angew. Chem., Int. Ed.* **2011**, *50*, 250.
- (22) Perry, R. H.; Brownell, K. R.; Chingin, K.; Cahill, T. J., III; Waymouth, R. M.; Zare, R. N. *Proc. Natl. Acad. Sci. U.S.A.* **2012**, *109*, 2246.
- (23) Xie, Y.; He, L. F.; Lin, S. C.; Su, H. F.; Xie, S. Y.; Huang, R. B.; Zheng, L. S. *J. Am. Soc. Mass Spectrom.* **2009**, *20*, 2087.
- (24) Miao, Z.; Chen, H.; Liu, P.; Liu, Y. *Anal. Chem.* **2011**, *83*, 3994.
- (25) Liu, P.; Lanekoff, I. T.; Laskin, J.; Dewald, H. D.; Chen, H. *Anal. Chem.* **2012**, *84*, 5737.
- (26) Nyadong, L.; Green, M. D.; De Jesus, V. R.; Newton, P. N.; Fernandez, F. M. *Anal. Chem.* **2007**, *79*, 2150.
- (27) Zhou, J.; Yao, S.; Qian, R.; Xu, Z.; Wei, Y.; Guo, Y. *Rapid Commun. Mass Spectrom.* **2008**, *22*, 3334.
- (28) Etter, M. C. *Acc. Chem. Res.* **1990**, *23*, 120.
- (29) Amendola, V.; Esteban-Gomez, D.; Fabbrizzi, L.; Licchelli, M. *Acc. Chem. Res.* **2006**, *39*, 343.
- (30) Costa, A. B.; Cooks, R. G. *Chem. Phys. Lett.* **2008**, *464*, 1.
- (31) Takats, Z.; Wiseman, J. M.; Cooks, R. G. *J. Mass Spectrom.* **2005**, *40*, 1261.
- (32) Pasilis, S. P.; Kertesz, V.; Van Berkel, G. J. *Anal. Chem.* **2007**, *79*, 5956.
- (33) Vekey, K.; Somogyi, A.; Wysocki, V. H. *J. Mass Spectrom.* **1995**, *30*, 212.
- (34) Wysocki, V. H.; Tsapralis, G.; Smith, L. L.; Breci, L. A. *J. Mass Spectrom.* **2000**, *35*, 1399.
- (35) Barbatti, M.; Aquino, A. J. A.; Lischka, H.; Schriever, C.; Lochbrunner, S.; Riedle, E. *Phys. Chem. Chem. Phys.* **2009**, *11*, 1406.